JOURNAL OF GUIDANCE, CONTROL, AND DYNAMICS
Vol. 24, No. 6, November–December 2001

Input/Output Conditioning of Robust Integrated Flight and Propulsion Controller

Matthew C. Turner,* Declan G. Bates,† and Ian Postlethwaite‡
University of Leicester, Leicester, England LE1 7RH, United Kingdom

We describe the application of a conditioning scheme to a linear integrated flight and propulsion control system for an experimental vertical/short takeoff and landing aircraft configuration in the transition (approach to hover) region of the flight envelope is presented. The proposed scheme guarantees satisfaction of limits on safety critical engine variables by using output conditioning to back off pilot demands in the event of a limit being encountered. Bounded-input/bounded-output stability results are presented for the resulting closed-loop system. At the plant input, an actuator linearization scheme is designed to minimize performance degradation due to backlash dynamics in the aircraft's thrust vectoring nozzles. The conditioning scheme also provides a mechanism for explicitly prioritizing requirements on flight-path angle over velocity in the case of engine performance limitations being reached. Performance and safety improvements due to the addition of the controller conditioning scheme are demonstrated in nonlinear simulation.

Nomenclature

$A(s)$	=	linear actuator dynamics
$C(s)$	=	actuator conditioning transfer function matrix
e	=	error signals
$G(s)$	=	plant transfer function matrix
$K(s)$	=	$\mathcal{H}^\infty$ loop-shaping integrated flight and propulsion control system
$T10$	=	high-pressure turbine stator outlet temperature, K
u	=	ideal control inputs
u_m	=	actual control inputs
Vt	=	velocity along the flight path, kn
v	=	compensation (back off) signal
$W(s)$	=	output conditioning transfer function matrix
z	=	controlled variables
α	=	aircraft angle of incidence, deg
γ	=	flight-path angle, deg
$\dot{\gamma}$	=	flight-path angle rate, deg/s
θ	=	pitch attitude, deg

I. Introduction

RESEARCH into the integration of aircraft flight and propulsion control systems is motivated by the desire to exploit potentially significant gains, both in terms of improved flying qualities and reduced pilot workload, which may be obtained by the use of propulsive system generated forces and moments for aircraft maneuvering in the low-speed region of the flight envelope. Recent advances in aircraft computer and actuator technologies allow a significant amount of extra control power to be generated via, for example, thrust vectoring and reversing nozzles, reaction control systems, air blowing/sucking devices, and so on. Successful integration of the flight and propulsion control systems is required to allow efficient use of these novel effectors for flight control, while simultaneously prohibiting violation of operational constraints dictated by engine safety considerations.

Whereas the most obvious current application of these new technologies is in the area of supermaneuverable vertical/short takeoff and landing (V/STOL) fighter aircraft,[1] these technologies also offer significant benefits to future civil commercial applications. Powered-lift flight capability could reduce aircraft structural weight and allow lower approach speeds, resulting in reduced runway length requirements, and integrated controls could improve flight safety by allowing for reconfiguration of damaged effectors.[2] Recent research into control technology requirements for future supersonic transport aircraft and hypersonic aerospacecraft have also indicated the necessity of fully integrating the airframe and engine controller design problems.[3,4]

Integration of the airframe and engine control systems results in significantly increased coupling between the two, heretofore largely independent, subsystems. In its simplest form, this coupling may be unidirectional (propulsive forces and moments affecting airframe states) but, in general, the use of novel effectors such as reaction control systems will also affect the engine operating point. Thus, systematic procedures for the design of integrated control systems are required that fully take into account the interactions between the various subsystems. Futhermore, because airframe and propulsion subsystems may have very different dynamic characteristics and may be designed, manufactured, and tested quite independently before being assembled into an overall system, any centralized integrated control strategy must be capable of being partitioned, to allow separate subcontrollers to address different control specifications in different parts of the system.[5]

In Ref. 6, a robust integrated flight and propulsion control (IFPC) system was designed for an experimental V/STOL aircraft configuration, using the method of $\mathcal{H}^\infty$ loop shaping. Results of piloted simulation trials with this centralized IFPC system are reported in Ref. 7, and a procedure for partitioning the IFPC system into lower-order engine and airframe subcontrollers is described in Ref. 8. In this paper, a conditioning scheme is presented that is wrapped around the previously designed IFPC system to meet certain performance and safety specifications that are difficult to address within a purely linear control framework. The paper is organized as follows. Section II briefly describes the V/STOL aircraft model and centralized IFPC system under consideration. Section III outlines the design and implementation of a nonlinear conditioning scheme to guarantee limits on safety critical engine variables, regardless of the demands input by the pilot. In Sec. IV, a pseudolinearizing conditioning scheme is applied to the aircraft's thrust vectoring nozzles to minimize performance degradation resulting from backlash dynamics. This scheme is used in combination with output conditioning to prioritize flight-path angle over velocity in the event of performance limits being exceeded. Improvements in performance and safety due to the controller conditioning scheme are demonstrated via nonlinear simulations in Sec. V. Finally, in Sec. VI, we offer some conclusions.

Received 29 June 2000; revision received 1 December 2000; accepted for publication 1 December 2000.

*Research Associate, Department of Engineering; mct6@sun.engg.le.ac.uk.
†Lecturer, Department of Engineering. Member AIAA.
‡Professor, Department of Engineering.

II. Linear Centralized IFPC System

The V/STOL aircraft concept considered in this study is representative of a next-generation Harrier-type vehicle, which naturally exhibits high engine/airframe interactions as well as a significant amount of interaxis coupling from control effectors to aircraft attitude/translational change. The airframe/engine interactions, interaxis couplings, and multiple safety limits require highly augmented control modes to ensure acceptable pilot workload in the powered-lift region of the envelope, for example, approach to hover. The Spey-wide envelope model (WEM) aircraft simulation model used in this study has been developed by the Defence Evaluation and Research Agency (DERA), to investigate various issues associated with the integration of flight and propulsion control systems for future V/STOL aircraft. The airframe model is based on the nonlinear DERA Bedford Harrier T.Mk4 WEM. This model has been used extensively in the vectored thrust aircraft advanced flight control (VAAC) Harrier research program[9] and has been established through flight trials as being an accurate representation of the real aircraft. This model is based around the well-known nonlinear rigid-body equations of motion

$$m\dot{U} = m(-WQ + VR) + F_x \tag{1}$$

$$m\dot{V} = m(-UR + WP) + F_y \tag{2}$$

$$m\dot{W} = m(-VP + UQ) + F_z \tag{3}$$

$$I_{xx}\dot{P} = I_{xz}(\dot{R} + PQ) + I_{xy}(\dot{Q} - PR) + I_{yz}(Q^2 - R^2) + (I_{yy} - I_{zz})QR + L \tag{4}$$

$$I_{yy}\dot{Q} = I_{xy}(\dot{P} + QR) + I_{yz}(\dot{R} - PQ) + I_{xz}(R^2 - P^2) + (I_{zz} - I_{xx})PR + M \tag{5}$$

$$I_{zz}\dot{R} = I_{yz}(\dot{Q} + RP) + I_{xz}(\dot{P} - QR) + I_{xy}(P^2 - Q^2) + (I_{xx} - I_{yy})PQ + N \tag{6}$$

where m represents the aircraft's mass; P, Q, R, U, V, and W represent the angular rates and linear velocities; the I_{ij} represent the aircraft's moments of intertia; and F_x, F_y, F_z, L, M, and N are the applied forces and moments generated by both aerodynamic and propulsion system effectors. Aerodynamic data generated from flight tests of the DERA VAAC Harrier are supplied in the form of lookup tables covering a flight envelople from −20 to +250 kn.

To provide an accurate representation of airframe/engine coupling, the airframe variables are integrated with a high-fidelity thermodynamic model (approximately 20 states) of the Rolls–Royce Spey engine, a two-spool reheated turbofan with the same basic architecture, for the purposes of control, as the EJ200, which is used to power the Eurofighter.[10] Nonlinear differential equations form the basis of this model, combined with lookup tables obtained from experimental data, and give a relatively faithful representation of the physical engine's behavior. Total thrust and high-pressure bleed flow to the reaction control system (RCS) is scaled to match Pegasus performance, and no duct losses are modeled in the rotating nozzles. The effect of high-pressure bleed flow (to the RCS) on the engine operating point is modeled, and the effect of front/rear thrust split on engine performance is assumed to be negligible. The engine model has a complex internal structure that prohibits an exhaustive description here. For more detail on aeroengine structure and control, see Ref. 11, for example.

The thermodynamic model of the Spey allows the control system designer full access to engine parameters, control being imparted through three actuators: exit nozzle area, main fuel flow, and inlet guide vane angles. Engine thrust is vectored through front and rear nozzle pairs, similar to the standard Harrier; however, for this aircraft concept the thrust applied to each pair can be independently varied and vectored. As another departure from the standard configuration, the front pair of nozzles have been moved forward and downward, displacing the center of thrust from the center of gravity and, thus, increasing thrust/pitch interactions.

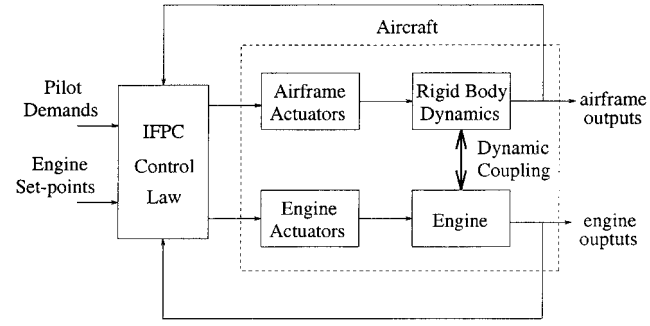

Fig. 1 Schematic of IFPC control architecture.

The overall Spey-WEM model consists of a dynamically coupled six-degree-of-freedom (6-DOF) rigid-body and engine system augmented with representative actuator dynamics and nonlinear limits, that is, rate and magnitude limits, yielding a total of 35 states. The nonlinear simulation model is believed to be valid over a flight envelope of −20 to +250 kn. A schemematic of the model architecture is shown in Fig. 1.

A centralized longitudinal-axis IFPC system was designed for the preceding airframe/engine configuration using the method of $\mathcal{H}^\infty$ loop shaping.[6] The design was carried out using a linearized model of the aircraft/engine dynamics, generated at the 80-kn transition region of the V/STOL flight envelope. At this point in the approach to hover, the aircraft is longitudinally unstable, and propulsion system generated forces and moments have largely taken over control of the aircraft from the conventional airframe effectors. The control law follows a two-inceptor strategy with fore/aft displacement of the center stick, producing a change in flight-path angle rate $\dot{\gamma} := \mathrm{d}/\mathrm{d}t(\alpha - \theta)$, and displacement of the left- hand pilot inceptor demanding aircraft velocity Vt parallel to this flight path. In addition, four safety critical engine variables [low-pressure compressor spool speed (NLPC), $T10$, high-pressure compressor surge margin (HPSM), and low-pressure compressor surge margin (LPSM)] and angle of attack α are directly controlled to respect specified safety limits. In this model, both high-pressure and low-pressure surge margins are assumed to be directly measurable. If this is not the case, these variables can be controlled indirectly by controlling other representative measurements, for example, the ratio of the compressor's static outlet pressure (at the bypass) to static inlet pressure.[12] Note that the specifications on the engine variables represent a hard limit. Performance (in terms of dynamic response to Vt or $\dot{\gamma}$ demands) is required to be sacrificed if this is necessary to keep these variables within their safety limits. More details of the control law requirements and design are given in Ref. 6. The controlled outputs and control inputs are summarized here:

$$z = \begin{bmatrix} \dot{\gamma} \\ Vt \\ \alpha \\ \text{NLPC} \\ T10 \\ \text{HPSM} \\ \text{LPSM} \end{bmatrix} \qquad u = \begin{bmatrix} \text{ETAD} \\ \text{ETASTK} \\ \text{FNOZ} \\ \text{RNOZ} \\ \text{SPLIT} \\ \text{MFF} \\ \text{ENOZA} \\ \text{IGVA} \end{bmatrix} \tag{7}$$

where ETAD is elevator position (−15–15 deg), ETASTK is pitch reaction control system position (−15–15 deg), FNOZ is front nozzle position (−5–120 deg), RNOZ is rear nozzle position (−1–120 deg), SPLIT is engine thrust split (0–1 dimensionless), MFF is main fuel flow (0–1.2 kg/s), ENOZA is exit nozzle area (0.8307–0.1602 sine petal angle), and IGVA is intel guide vane angle (−8–35 deg).

Robustness and handling qualities characteristics of the centralized IFPC system were evaluated in piloted simulation trials at DERA Bedford's Real Time All Vehicle Simulator facility and reported in Ref. 7. Level 1 or 2 flying qualities were attained for maneuvers in Vt and $\dot{\gamma}$ over the 50–110 kn region of the flight envelope. Although the overall performance of the IFPC system was found to

be very satisfactory, three particular problems were identified in the course of the trials.

1) Although the controlled engine variables were generally kept close to their nominal values, aggressive pilot demands in Vt or $\dot{\gamma}$ could result in some or all of them transiently exceeding their specified safety limits.

2) Backlash in the dynamics of the front and rear thrust vectoring nozzles had a significant effect on the achieved flying qualities. In particular, they made it very difficult to meet the specification on decoupling between Vt and γ, which allows a maximum deviation of 0.3 deg in γ during Vt maneuvers.

3) The IFPC system provided no means of explicitly prioritizing flight path over velocity demands, an important requirement in performance limited situations at this point in the V/STOL flight envelope.

Clearly, all of the preceding issues are difficult to address in the context of a purely linear controller design. The tradeoff between satisfaction of performance specifications on Vt and $\dot{\gamma}$ and respecting limits on safety critical engine variables is managed in the linear design via selection of the $\mathcal{H}^\infty$ weighting functions. This tradeoff is set to keep engine variables within their limits only for certain assumed levels of pilot demands because complete decoupling of these variables from large dynamic thrust changes is not physically possible (or desirable, because it would produce seriously degraded thrust response characteristics). Indeed, no sensible linear control system can guarantee hard limits on all of its controlled variables for arbitrary reference demands. Also, whereas certain types of actuator nonlinearities such as rate and saturation limits can be taken into account by carefully shaping the control signal bandwidths and magnitudes, nonlinear behavior from dead zones and backlash is very difficult to address explicitly in the context of a linear controller design. Finally, the requirement to prioritize flight-path angle over velocity (but only in the event of a performance limit being reached) obviously also requires some additional control logic in addition to that provided by the basic linear IFPC system. The design and implementation of a conditioning scheme to address all of the preceding issues is described in the remainder of this paper.

III. Output Conditioning to Guarantee Engine Safety Limits

The literature is fairly devoid of methodologies that can cope with hard constraints on the controlled outputs of a feedback system. Possibly the first and most widely applied method is override control.[13] This approach deals with the case of ensuring a secondary controlled variable does not exceed its limit while the primary controlled variable is controlled. In the event of a limit violation, the control input to the plant is altered to bring the secondary variable back within its limits. This approach is closely related to the ideas of multimode control,[14] where each controller is designed to enforce different (conflicting) design criteria, and switching logic is used to decide which controller is on-line at a given time.

There are many industrial applications of the two preceding methods, with current engine control systems often using variants of these techniques to enforce output limits. The main problem with such approaches is that they break the nominal linear closed loop to compensate in the event of an output violation. This not only has implications for closed-loop stability, particularly with switching schemes, but can also compromise transient performance. Furthermore, although such compensators may be straightforward to design in the single input/single output (SISO) case, the difficulty increases greatly for multivariable systems. Finally, we note that schemes of the type just described are usually implemented purely within the context of the engine control problem and do not easily allow for efficient integration of the flight and propulsion control problems.

Another approach is that of Ref. 15, where a reference governor is used to ensure that limits are not violated. This approach applies to both input and output constraints and seems to offer an attractive solution. However, the resulting mathematical programming problem is computationally intensive, and, for the IFPC system considered here, which has high dimensionality, its application is not feasible.

In Ref. 8, a scheme was proposed in the context of partitioned IFPC systems, whereby safety limits on critical engine variables were reflected back to form extra constraints on the engine actuators. Although this scheme was seen to perform well, antiwindup conditioning logic is then required to ensure that closed-loop stability and performance is maintained in limited situations.

In this paper we consider a different approach to the problem, which avoids compromising the stability of the original closed-loop and can be applied in the context of a full IFPC system. The method is based on similar ideas to classical antiwindup schemes[16] and, to the authors' knowledge, first appeared explicitly in Ref. 17. The method is particularly suited to the plant we consider here for several reasons. First, it guarantees bounded-input/bounded-output stability for a large class of compensator choices. This is something that override control cannot conveniently do for this system because stability in that paradigm relies on the circle or Popov criteria.[18] Because the linear plant–controller combination considered here is ill conditioned (by design, because tighter control of airframe variables than engine variables is required), has a high dimensionality, and possesses multiple inputs and outputs, such tests have to be performed as a set of linear matrix inequality (LMI) conditions, which is difficult for such a plant. Second, as will be seen, the scheme itself is relatively simple and, thus, more convenient to implement than the reference governor scheme of Ref. 15.

The conditioning scheme, referred to as output antiwindup in Ref. 17, is shown in Fig. 2. $K(s)$ and $G(s)$ represent the controller and plant, and their interconnection forms the primary control loop. Around them is another loop containing a deadzone, which models the output limits, and linear compensator $W(s)$, which is designed such that a graceful degradation of performance occurs when output limits are violated. The saturation element is added to ensure only bounded signals are input into the primary control loop. The operation of the scheme is as follows. The system behaves as the nominal linear system, providing the output vector, $\boldsymbol{y} \in \mathbb{R}^p$, remains within the deadzone. However, if the output vector strays outside the deadzone, the outer-loop will become active. This has the effect of modifying or backing off the reference demands. The compensator $W(s)$ is designed such that this will result in the output being regulated back below its limit (i.e., so that its value remains within the deadband), in such a way that the effect on performance experienced by the pilot is minimized. Thus, nominal linear performance is maintained where possible, with the compensator $W(s)$ only taking action if a limit is exceeded. This enables linear controllers to be designed for high performance, with a performance degradation only occuring when limits are violated.

The stability of such a scheme was proved using the monotone small gain theorem in Ref. 17. Here we provide a simpler proof using elementary principles. Let the saturation function, $\mathrm{sat}_{\bar{z}}(.)$: $\mathbb{R}^q \to \mathcal{Q} \subset \mathbb{R}^q$, be a globally Lipschitz operator defined as

$$\mathrm{sat}_{\bar{z}}(z) := \begin{bmatrix} \mathrm{sat}_{\bar{z}_1}(z_1) \\ \mathrm{sat}_{\bar{z}_2}(z_1) \\ \vdots \\ \mathrm{sat}_{\bar{z}_p}(z_p) \end{bmatrix} \tag{8}$$

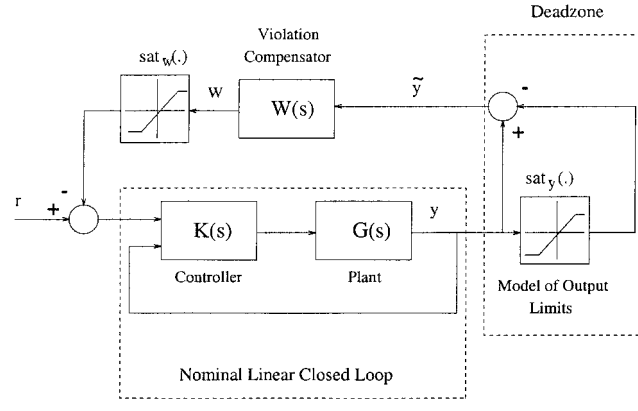

Fig. 2 Output conditioning scheme.

where $\text{sat}_{\bar{z}_i}(z_i) := \text{sign}(z_i)\min\{|z_i|, \bar{z}_i\}$. Note that $\mathcal{Q}$ is, thus, a compact subset of $\mathbb{R}^q$ and can be described as

$$\mathcal{Q} = [-\bar{z}_1, \bar{z}_1] \times [-\bar{z}_2, \bar{z}_2] \times \cdots \times [-\bar{z}_q, \bar{z}_q] \subset \mathbb{R}^q \tag{9}$$

Then the deadzone can be defined as

$$Dz_{\bar{z}}(\boldsymbol{z}) := \boldsymbol{z} - \text{sat}_{\bar{z}}(\boldsymbol{z}) \tag{10}$$

Using the preceding definitions, we have the following theorem.

Theorem 1: Consider the system in Fig. 2, and assume that $K(s)$ stabilizes $G(s)$. Furthermore, assume the system is mathematically well posed; that is, for every input $\boldsymbol{r}$, there exists a unique output $\boldsymbol{y}$. Then, for all $\bar{\boldsymbol{w}}_i \in [0, \infty)$, the system is bounded-input/bounded-output (BIBO) stable, where $\bar{w}$ represents the limits of the saturation function.

Proof: We must prove that for every bounded input, the output y is also bounded. First note that our well-posednature assumption guarantees existence and uniqueness of solutions. Next, because $K(s)$ stabilizes $G(s)$, the nominal linear closed loop $G_c(s)$ is, thus, asymptotically stable; that is, all of its poles lie in the open left half-plane. Next, because $\bar{\boldsymbol{w}}_i < \infty$, the signal $\text{sat}_{\bar{w}}(w)$ is, thus, bounded. Because $\boldsymbol{r}$ is bounded, $\text{sat}_{\bar{w}}(w)$ is bounded, and $G_c(s)$ is asymptotically stable, it thus follows that $\boldsymbol{y}$ is bounded. Hence, the system is BIBO stable. □

In fact, this theorem holds for a wider class of functions than simply the saturation and deadzone nonlinearities. The key requirement is that these functions be Lipschitz continuous, bounded operators. That is, a Lipschitz operator with bounded $\mathcal{Q}$ (in the definition of the saturation function) is sufficient. For example arctan(.) or tanh(.) could be used in place of the saturation function, and one of these functions subtracted from the identity operator could be used in place of the deadzone.

This stability result is not as strong as asymptotic stability (which can be guaranteed by the Circle or Popov criteria) and, thus, cannot guarantee the absence of limit cycles. However, it does guarantee that asymptotically divergent trajectories are not encountered, giving a pilot some time to manually recover in the event of a limit cycle. Besides, judicious choice of the parameters $W(s)$, $\bar{w}$, and $\bar{y}$, which in the authors' experience has been easy, will yield asymptotic stability for most r. A mathematically well-posedness is guaranteed if the direct feedthrough term of either $G_c(s)$ or $W(s)$ is zero.[19] The strength of the scheme's simplicity is, thus, enhanced by its BIBO stability guarantees. In fact, these two facets are crucial to its implementation in the IFPC context considered here, where the already high complexity and high dimensionality prohibits complicated conditioning schemes, both from numerical and on-line computational points of view.

Figure 3 shows the diagram of the output conditioning scheme used to back off $\dot{\gamma}$ demands in response to engine limit violations. Because the linear closed-loop, by virtue of the linear controller, exhibited a decoupled structure, $W(s)$ was chosen as the transfer function matrix (from engine limits to $\dot{\gamma}$ demand):

$$W(s) = [w_{\text{NLPC}}(s) \quad w_{T10}(s) \quad w_{\text{HPSM}}(s) \quad w_{\text{LPSM}}(s)] \tag{11}$$

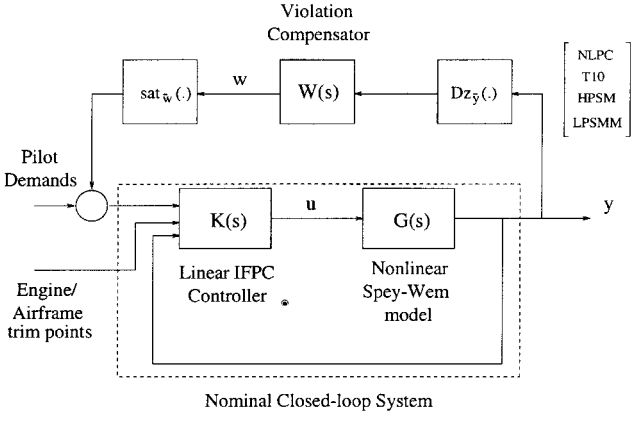

Fig. 3 Output conditioning for guaranteed engine safety limiting.

Because the objective was to keep the structure as simple as possible, it was found that choosing

$$w_{T10}(s) = 1.5s/(0.5s + 1) \tag{12}$$

$$w_{\text{NLPC}}(s) = w_{\text{HPSM}}(s) = w_{\text{LPSM}}(s) = w_{T10}(s) \tag{13}$$

gave an acceptable response when output violation was encountered because the dynamics of the variables are similar. Some iteration was required, and such choices do not constitute optimal values (some standard optimization procedures, such as $\mathcal{H}^\infty$ and LMI optimization, will fail for this plant due to its poor numerical conditioning and high dimensionality). Iteration, however, proved to be fairly easy: high gains corresponded to large back offs and low-high-pass filtering corresponded to decreased/increased high-frequency activity in the compensation signal. The deadband associated with each limit was chosen just within its maximum and minimum output limits (the deadzone associated with $T10$ was chosen as $[-1425, 1425]$, the lower limit being redundant) to ensure the outputs never reached their limits. Recall that any finite saturation value would guarantee BIBO stability, but obviously a large bounded output is undesirable. Hence, it was decided to limit the magnitude of the back-off signal from engine variables to $\dot{\gamma}$ at 10 deg/s. A well-posedness was guaranteed in this case because the linear closed loop contained no direct feedthrough term. A scheme to back off Vt demands in the case of engine limit violations was designed in a similar manner.

IV. Nonlinear Conditioning for Improved Vt/γ Performance

This section builds on the ideas of the last by employing the same type of output conditioning to prioritize satisfaction of flight-path specifications over velocity demands in performance limited situations, but also embellishes this through the use of an actuator conditioning scheme. The particular problem addressed is the excessive coupling into γ allowed by the linear IFPC system, when an aggressive demand on Vt is injected by the pilot in nonlinear simulation.

The first step is to design the back-off scheme in a similar manner to the engine limiting scheme, the idea being not to sacrifice performance in Vt unless a violation of a specification on γ occurs. With reference to Sec. II, note that the performance specifications require coupling into γ for any velocity maneuvers to be below 0.3 of a degree: a very stringent demand. Unlike the engine violation problem that could be investigated easily on the linear model, because it is a direct consequence of two conflicting criteria, the situation with the γ coupling is more complicated because γ stays well within the required limits for velocity maneuvers in linear simulation. In fact, as noted by the pilots in Ref. 7, the coupling into γ is the result of a fairly complex interplay between the nonlinear interactions in the engine/airframe model and the backlash present in the aircraft's thrust vectoring nozzle actuators (to be discussed later). Hence, the design of a conditioning scheme to alleviate this problem was heavily tied to nonlinear simulations.

The output conditioning loop was created, as per Fig. 2, with the loop backing off the Vt reference demand when excessive coupling into $\dot{\gamma}$ occurred. The loop could not be between γ and Vt because γ is the integral of $\dot{\gamma}$, which would mean the eigenvalues of $G_c(s)$ would be in the closed, rather than open, left half-plane, thus compromising the stability guarantees. This complicated the choice of the deadzone because the $\dot{\gamma}$ coupling allowed had to reflect the γ coupling specifications. When the deadband was set as the interval $[-0.3, 0.3]$, however, satisfactory results were produced. The compensator $w_\gamma(s)$ was chosen as the simple transfer function

$$w_\gamma(s) = 80/(s + 1) \tag{14}$$

that is, a high-gain, low-pass filter. This prevented high-frequency back-off activity, which was seen to cause a general performance degradation due to excitation of actuator rate limits. The saturation limits of the back-off signal associated with this conditioning loop were more difficult to choose than with the engine conditioning loop.

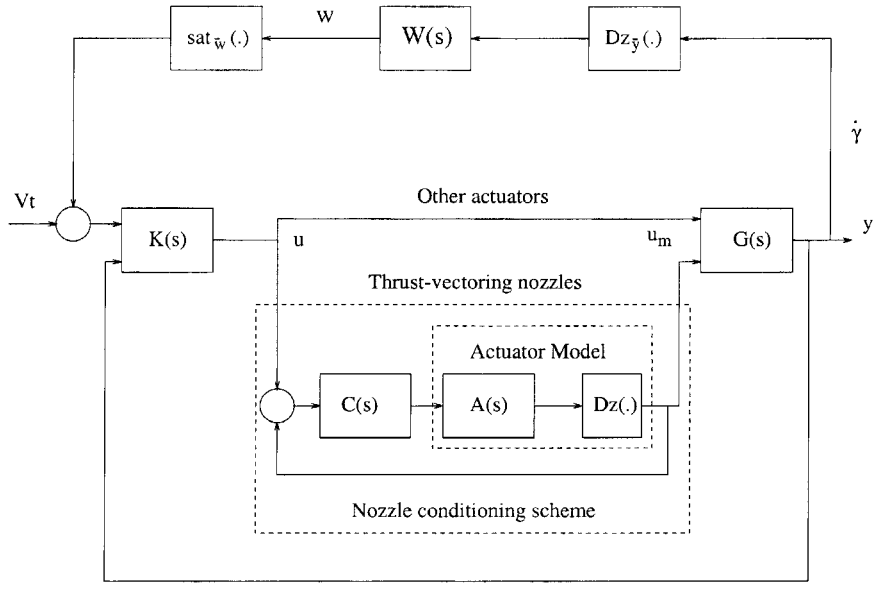

Fig. 4 Actuator linearization and conditioning for γ prioritization.

For satisfactory backing off of small demands, the gain in $W(s)$ had to be large, but, because the coupling into γ increased nonlinearly with increased Vt demand, for large Vt demands excessive back off was observed. Hence, to avoid this, the compensation signal was saturated fairly severely at ± 10 kn. An alternative to this would be the use of a nonlinear gain, although guarantees of stability would then be harder to obtain.

Recall that the output conditioning scheme assumes that the closed-loop combination of the plant and controller is linear. This implicitly assumes actuator linearity, which is obviously not the case here. Although the linear controller was designed such that, generally, no actuator magnitude or rate limits were encountered, a backlash of significant magnitude is present in the aircraft's thrust vectoring nozzles. Because the nozzles are primary actuators for satisfying demands on Vt, this behavior significantly impaired the conditioning scheme's performance when small demands (less than 10 kn) were made. Put another way, the back-off signals sent to the reference were not fully passed on to the plant due to the backlash residing in each of the nozzles. To improve the operation of the scheme, conditioning logic was designed to linearize the behavior of these effectors.

The control literature is abundant with conditioning schemes for systems with actuator magnitude, and possibly rate, limits. This is not surprising because this type of nonlinearity is perhaps the most prevalent in practice, and in certain applications disregard for such nonlinear phenomena can cause severe performance degradation and often instability or limit cycling. There are many antiwindup schemes, of varying complexity, available to deal with such actuator nonlinearites. The basic mechanism by which most work is to reduce the magnitude, and possibly direction in the multivariable case, of the control signal until it falls below the saturation limits, after which normal operation can resume. However, when such schemes are applied to actuators that are also subject to other types of nonlinearites, specifically a deadzone or backlash, the performance is often far from desirable. For instance, in the case of a deadzone, many antiwindup schemes, such as the classical high-gain technique, attempt to keep the control signal at its deadzoned value. Thus, if the control signal starts at zero, the antiwindup scheme attempts to keep the signal entering the plant zero for all time, resulting in essentially open-loop behavior.

The aim here is to develop a simple technique for conditioning the nonlinear aircraft nozzles. Because the linear controller ensured magnitude/rate limits were rarely encountered, the primary goal was to ameliorate the effects of the backlash present in the thrust-vectoring nozzles. The nozzles have a fairly complex structure: They are modeled by two second-order transfer functions (modeling the hydraulics and nozzle dynamics, respectively) connected on either side of a backlash nonlinearity (due to mechanical linkages). For the design of the conditioning scheme, they are approximated as a fourth-order transfer function in series with a deadzone of ± 6 deg, that is, we neglect the hysteresis dynamics. This allowed considerable complexity to be avoided, without significantly compromising the performance of the linearization scheme.

The approach adopted is similar to classical actuator controller design procedures. Consider Fig. 4, which shows a simple conditioning scheme for an actuator consisting of a deadzone and linear dynamics $A(s)$. The transfer function $C(s)$ represents a compensator, to be designed, that improves the performance of the raw actuator. The output of the controller, the ideal control signal, is u, and the actual input to the plant, which is assumed to be available for feedback, is u_m. This is a standard assumption in the antiwindup literature; if u_m is not available for feedback, a software model can be used instead. Obviously, for nominal performance the requirement is that $u_m = u$.

To understand the functionality of the conditioning scheme, an approximation is considered. Note that the deadzone is a static nonlinearity with gain $\beta \in [0, 1)$, that is, for each fixed-amplitude input, the gain of its input–output map is a member of the semiclosed unit interval (strictly less than unity). Hence, with this approximation it follows that

$$u_m(s) = \left[\frac{\beta A(s)C(s)}{1 + \beta A(s)C(s)}\right] u(s) \tag{15}$$

From this it can be easily seen that if $C(s)$ is large, then $u_m(s) \approx u(s)$, providing $\beta \neq 0$. This is reminiscent of the high-gain approach to antiwindup, the major difference being that the high gain here resides in the forward path. The reason for this is that if the high gain was placed in the feedback path, the compensator would try to make u_m equal to u after it has passed through the deadzone; for small inputs this would, thus, mean u_m would start and remain at zero. By the placing of the high gain in the forward path, for a small signal, amplification takes place before the deadzone is encountered, meaning that the deadband is avoided. The stability of the system is easier to guarantee than the output conditioning scheme because the deadzone conditioning is only performed around one actuator. Hence, stability can be guaranteed easily by the Popov or Circle criteria (in the SISO case, simple graphical tests are available). Furthermore, because this conditioning only considers the actuators, the complexity is fairly low and, thus, optimization methods can be used if necessary. Because, in effect, the closed loop is also being

altered, the stability of the resulting closed loop with conditioned actuators must also be considered. For this plant, this is a more difficult problem. One point of view is that the conditioned actuators behave in an almost linear fashion and, hence, their inclusion in the closed loop is less likely to have serious stability implications than the pure deadzone.

The only parameter to be designed for the conditioning scheme is the transfer function $C(s)$. A naive way of doing this would be to just choose $C(s)$ as a large gain, to make u_m as close to u as possible. However, unless the linear dynamics are fairly benign (which, admittedly, is often the case), this is impossible because for large gains the root locus of the open-loop system may stray into the right half complex plane. For the case considered here, designing $C(s)$ correctly was important. Both the front and rear nozzles had fourth-order transfer functions of the following form for their linear part:

$$A(s) = \left[w_1^2 \big/ \left(s^2 + 2\zeta_1 w_1 s + w_1^2\right)\right] \cdot \left[w_2^2 \big/ \left(s^2 + 2\zeta_2 w_1 s + w_2^2\right)\right] \tag{16}$$

with natural frequencies $w_1 = 11.9$ and $w_2 = 10.5$ rad/s and damping ratios $\zeta_1 = 0.96$ and $\zeta_2 = 0.47$. The root locus of this function is shown in Fig. 5. The locus crosses into the right half-plane at approximately a gain of 1.7, making it clear that using a pure high gain for $C(s)$ is not plausible. Instead $C(s)$ was designed using $\mathcal{H}^\infty$ optimization to minimize the $\mathcal{H}^\infty$ norm of the transfer function between the nominal control signal u and the error $u - u_m$. Furthermore, because the control activity would be concentrated

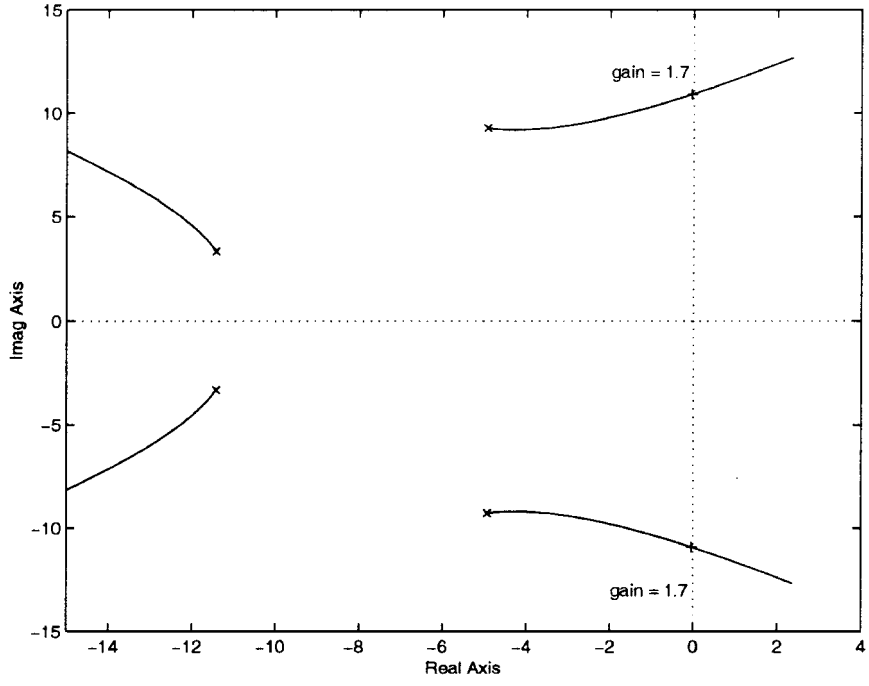

Fig. 5 Root locus of linear dynamics of thrust vectoring nozzles.

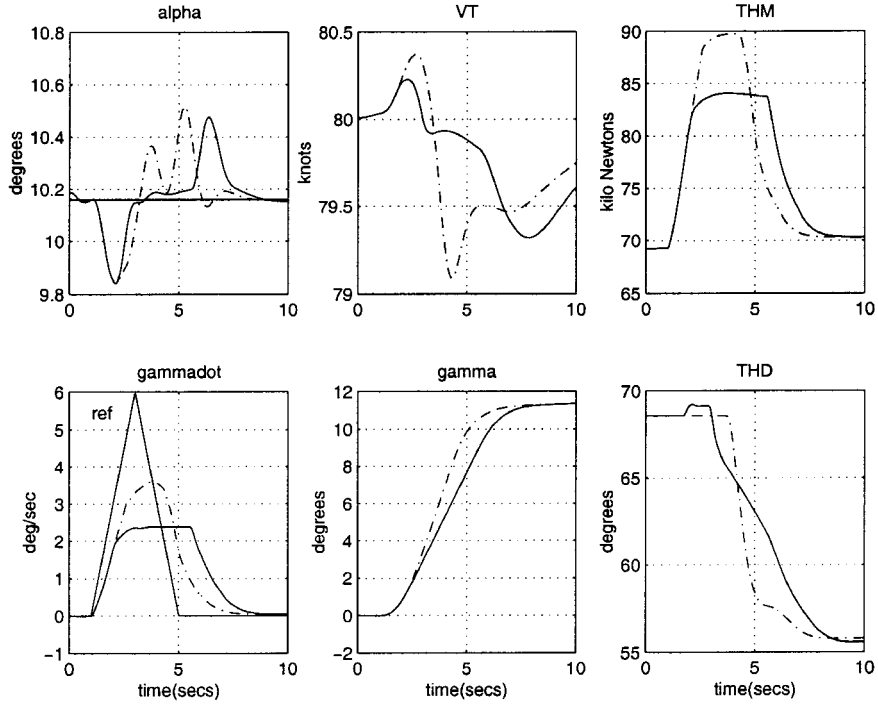

Fig. 6 Airframe responses to $\dot{\gamma}$ demand (——, conditioned response; –·–, unconditioned response).

in the low-frequency range, this was weighted by the low-pass filter

$$W_e = 4/(s + 0.01) \tag{17}$$

To ensure a properly posed optimization problem, this was constrained by simultaneously minimizing the $\mathcal{H}^\infty$ norm from u to the output of $C(s)$, weighted by $W_2 = 0.01$. In this way a fifth-order compensator with $\mathcal{H}^\infty$ norm ≈ 0.25 was synthesized for both front and rear nozzle conditioning (in practice, these compensators could probably be model reduced). Becuase of the presence of the deadzone nonlinearity, stability of this scheme was not guaranteed a priori, but postsynthesis analysis via the Popov criterion revealed that stability of the scheme was indeed guaranteed. Moreover, the $\mathcal{H}^\infty$ synthesis ensured that some robustness to uncertainty in the nozzles dynamics, such as the neglected hysteresis, is achieved. Finally, because the transfer function $A(s)$ contained no direct feedthrough term, the well-posedness of the overall conditioning scheme was ensured.

Note that $\mathcal{H}^\infty$ optimization could be used to guarantee robust stability of the actuator conditioning scheme by treating the deadzone as a linear gain plus uncertainty (which, in this case, would be

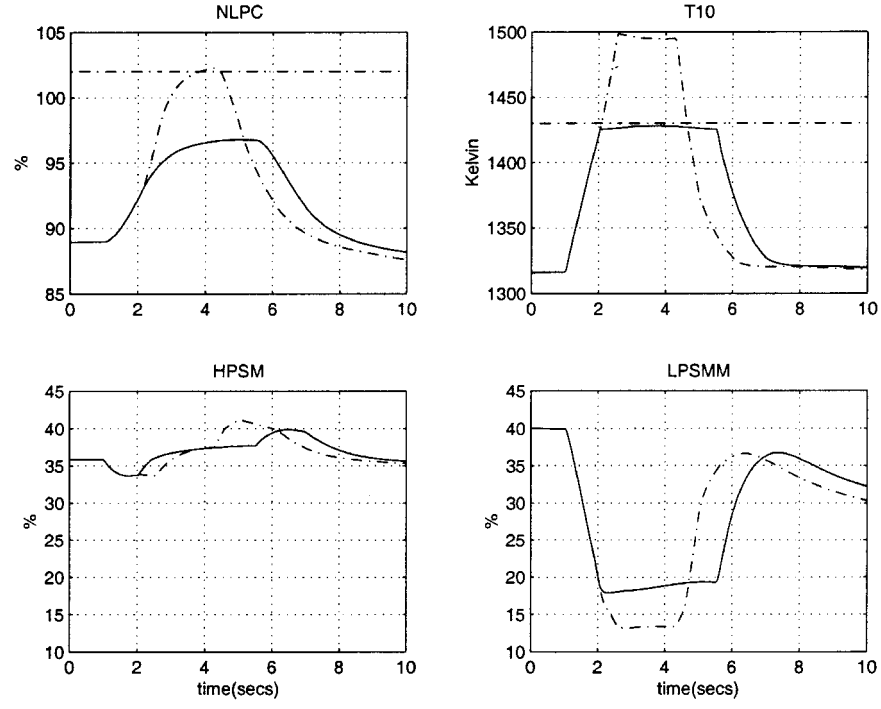

Fig. 7 Engine responses to $\dot{\gamma}$ demand (——, conditioned response; –·–, unconditioned response).

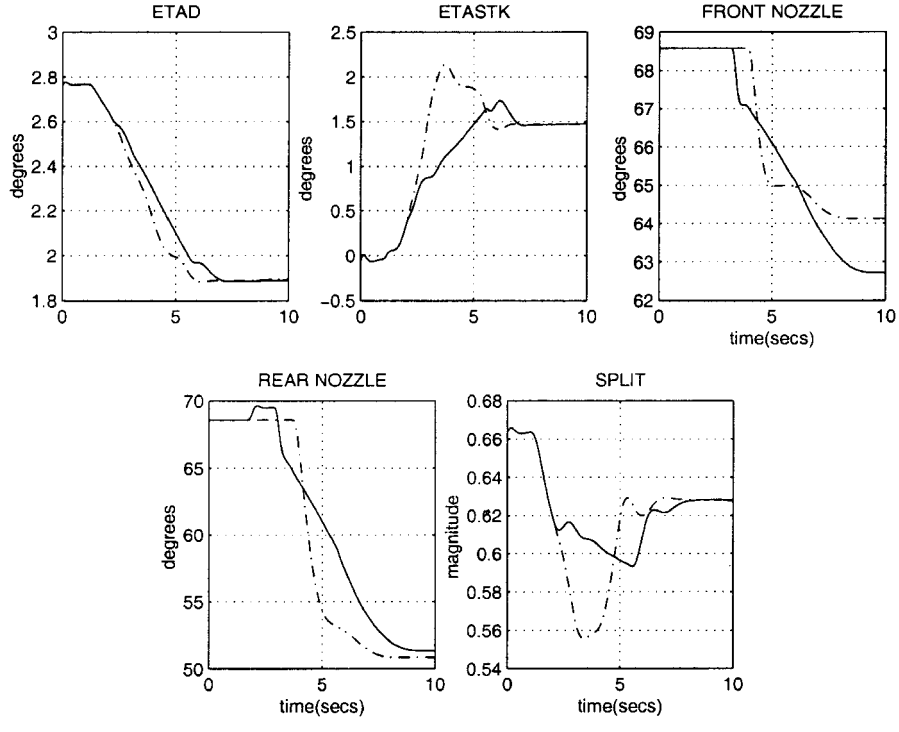

Fig. 8 Airframe actuators for $\dot{\gamma}$ demand (——, conditioned response; –·–, unconditioned response).

the saturation function). Stability could then be obtained by a small gain condition.[18] Because of the conservatism of this test, however, such a result would not commonly allow the gain of $C(s)$ to be high enough to achieve satisfactory performance; hence, we have resorted instead to the less conservative Popov criteria to guarantee stability because this does not necessarily preclude the use of high gains.

V. Nonlinear Simulation Results

Although the conditioning schemes were conceived essentially for linear systems with isolated saturation and deadzone nonlinearities, their practical worth is tested through full nonlinear simulation, with inceptor demands corresponding to pilot maneuvers executed in Ref. 7 being used in all cases.

Figures 6–9 show the aircraft responses to an aggressive demand in $\dot{\gamma}$. Note that with the unconditioined IFPC system the high-pressure turbine stator outlet temperature $T10$ exceeds its limit by 75 deg. Also, the control signals in the engine actuators MFF and ENOZA saturate at their upper limit. Conversely, the conditioned response respects all limits: $T10$ does not exceed its limit, and the engine actuators do not saturate, even though they are not explicitly conditioned themselves. Some small loss of performance is incurred, with the $\dot{\gamma}$ response not achieving such a high magnitude, although γ reaches its desired value, albeit more slowly. Note that

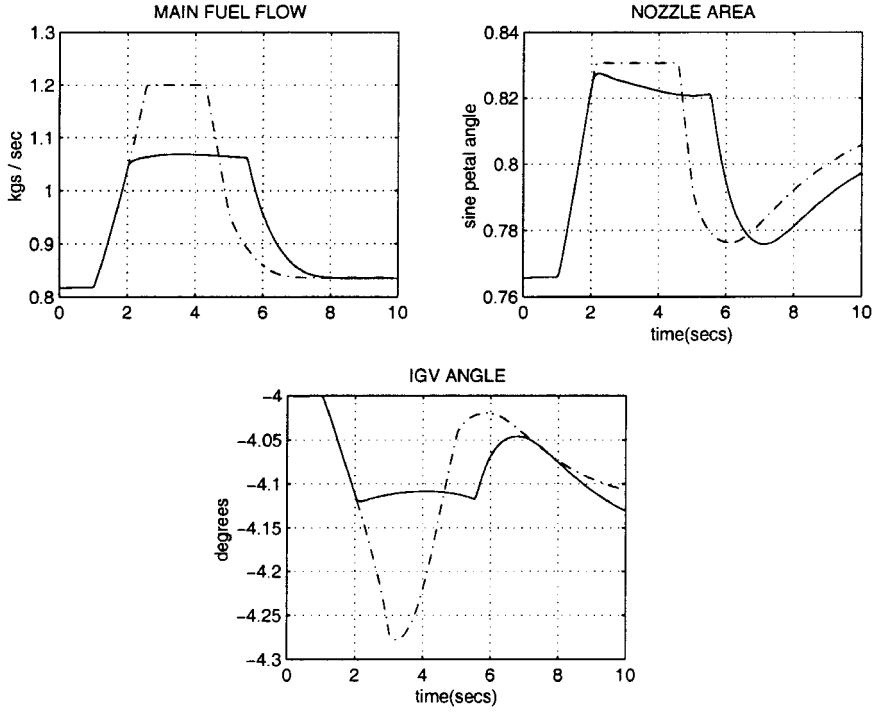

Fig. 9 Engine actuators for $\dot{\gamma}$ demand (——, conditioned response; –·–, unconditioned response).

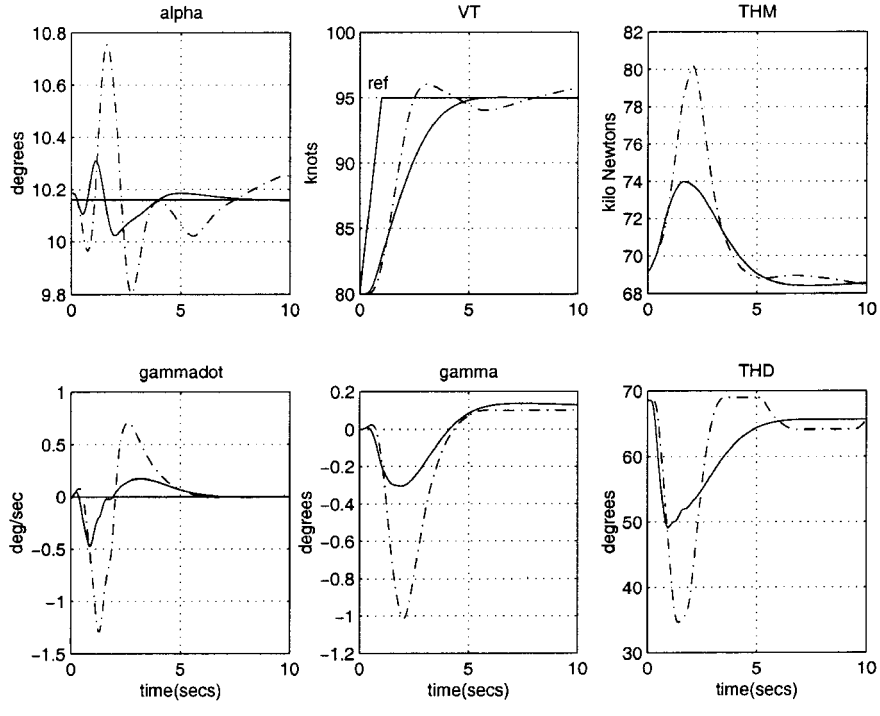

Fig. 10 Airframe responses to 15-kn Vt demand (——, conditioned response; –·–, unconditioned response).

the conditioning backs off the $\dot{\gamma}$ demand, preventing such a large rate from being obtained. This back off in demand then causes the temperature $T10$ not to exceed its limit and also prevents the actuators saturating.

Figures 10–13 depict the system's response to a 1-s ramp demand, of magnitude 15 kn, in Vt. Note that without conditioning, the coupling into γ is approximately three times its allowable limit, whereas with the conditioning scheme the coupling is safely inside its 0.3-deg boundary. Some rise time has been sacrificed in the Vt response. Note how the backed off demand causes Vt to follow a slower ramp when the conditioning scheme becomes active. However, the response with the conditioning scheme generally appears smoother with less overshoot, partly due to the nozzle linearization scheme.

Finally, Fig. 14 shows some responses to a step demand of 5 deg in Vt. The purpose of Fig. 14 is to illustrate the difference the actuator linearizing scheme makes for small demands, where, of course, the deadzone in the nozzles causes the most disruption. For comparison purposes, the response of the nonlinear model with all linear actuators is also shown. It is clear that the behavior of the system with linearized actuators is similar, almost identical in some variables, to that of the system with linear actuators. The response of

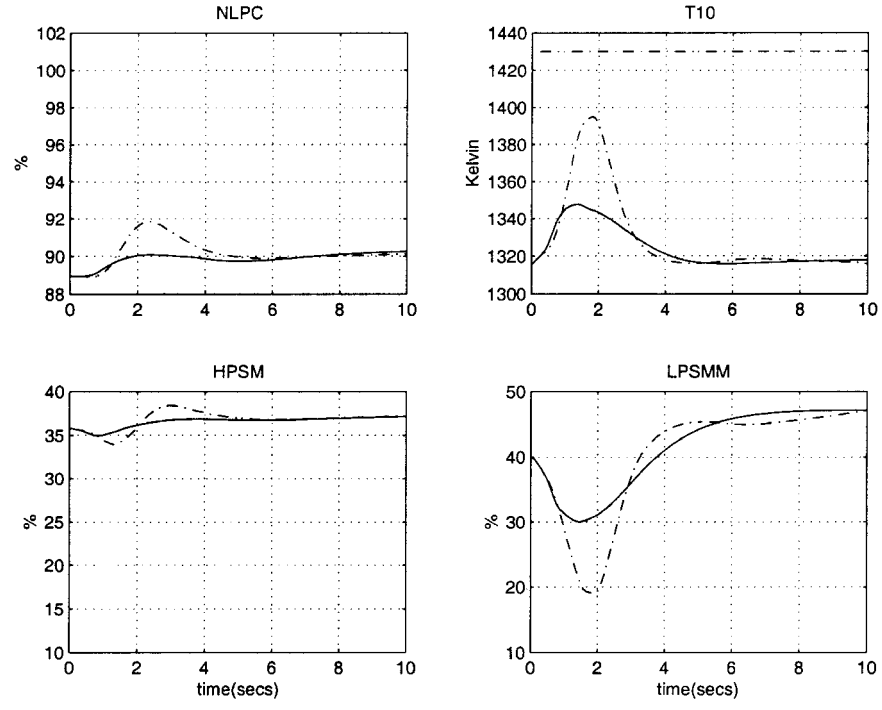

Fig. 11 Engine responses to 15-kn Vt demand (——, conditioned response; –·–, unconditioned response).

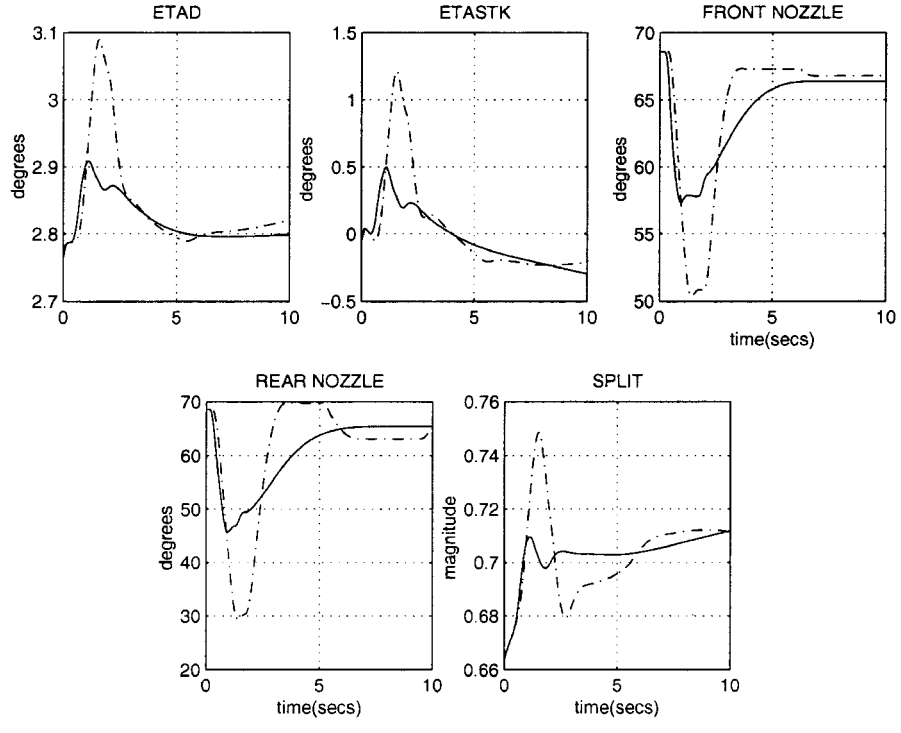

Fig. 12 Airframe actuators for 15-kn Vt demand (——, conditioned response; –·–, unconditioned response).

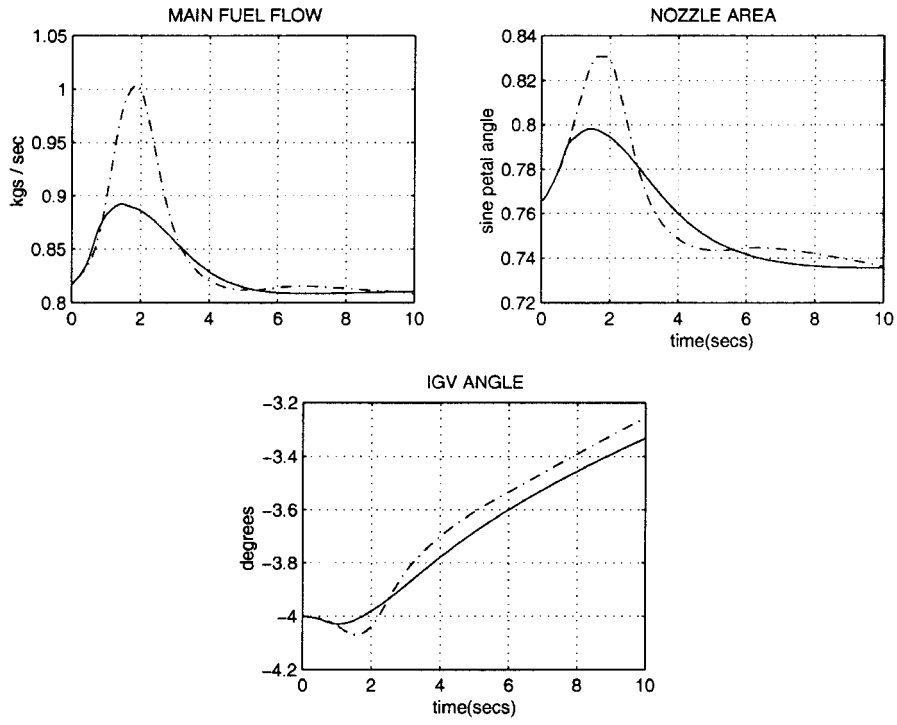

Fig. 13 Engine actuators for 15-kn *Vt* demand (——, conditioned response; –·–, unconditioned response).

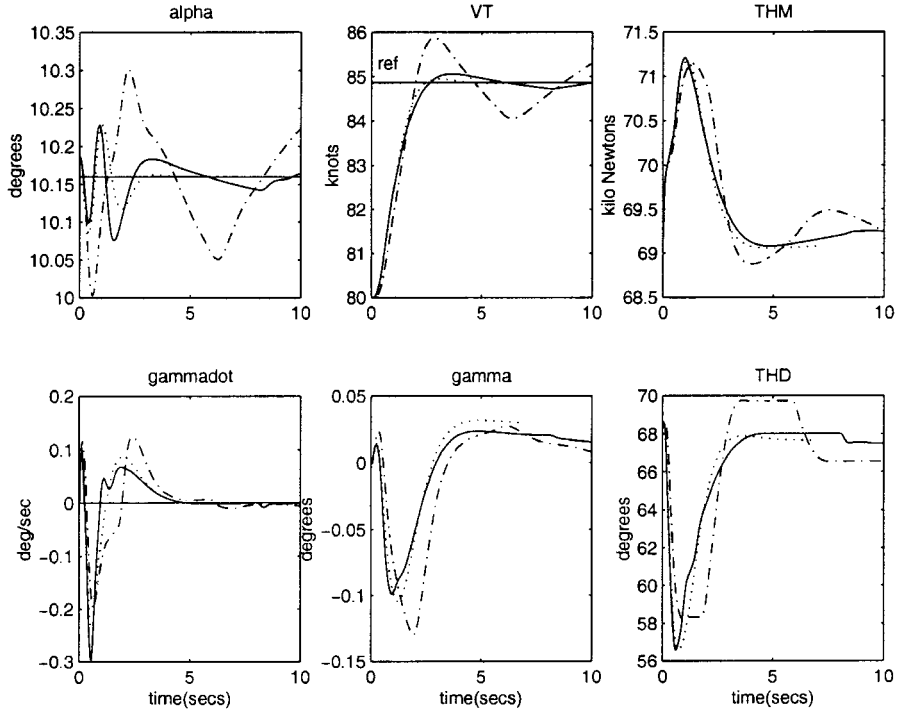

Fig. 14 Airframe responses to 5-kn *Vt* demand (——, conditioned response; –·–, unconditioned response).

the system with the unconditioned nonlinear actuators is considerably worse, with *Vt* exhibiting excessive overshoot and a prolonged damped oscillation.

VI. Conclusions

This paper has presented some methods for conditioning linear control systems to deal with essentially nonlinear performance and safety issues. With these methods, a conditioning scheme was designed and implemented on a linear integrated flight and propulsion control system for an experimental V/STOL aircraft model. The conditioning scheme guarantees satisfaction of limits on safety critical engine variables by using output conditioning to dynamically back-off pilot demands in the event of a limit being encountered. Conditioning was also designed to minimize performance degradation due to nonlinear behavior in the aircraft's control effectors and to provide a mechanism for explicitly prioritizing requirements on flight-path angle over velocity in the case of engine performance limitations being reached. Performance and safety improvements due to the addition of the conditioning scheme were demonstrated in nonlinear simulation. The proposed approach provides a transparent and powerful mechanism for addressing nonlinear actuator dynamics and control specifications within the framework of robust integrated flight and propulsion control system design.

Acknowledgments

The authors would like to acknowledge the United Kingdom Engineering and Physical Sciences Research Council for financial support and Defence Evaluation and Research Agency Bedford for providing the simulation model of the vertical/short takeoff and landing aircraft. The authors are also indebted to Sarah Gatley of the University of Leicester and Melker Harefors of Volvo Aero Corporation for several useful discussions during the course of this work.

References

[1]Wise, K. A., "Applied Controls Research Topics in the Aerospace Industry," *Proceedings of the IEEE Conference on Decision and Control*, Vol. 1, IEEE Publications, Piscataway, NJ, 1995, pp. 751–756.

[2]Bennani, S., van der Sluis, R., Schram, G., and Mulder, J. A., "Control Law Reconfiguration Using Robust Linear Parameter Varying Control," *Proceedings of the AIAA Conference on Guidance, Navigation, and Control*, Vol. 2, AIAA, Reston, VA, 1999, pp. 977–987.

[3]Burcham, F. W., Gilyard, G. B., and Gelhausen, P., "Integrated Flight–Propulsion Control Concepts for Supersonic Transport Airplanes," *SAE Transactions*, Vol. 14, Pt. 2, 1990, pp. 26–33.

[4]Schmidt, D. K., "Dynamics and Control of Aeropropulsive/Aeroelastic Hypersonic Vehicles," *Proceedings of the AIAA Conference on Guidance, Navigation, and Control*, AIAA, Washington, DC, 1992, pp. 859–871.

[5]Garg, S., "Partitioning of Centralised Integrated Flight/Propulsion Control Design for De-Centralised Implementation," *IEEE Transactions on Control Systems Technology*, Vol. 1, No. 2, 1993, pp. 93–100.

[6]Bates, D. G., Gatley, S. L., Postlethwaite, I., and Berry, A. J., "Integrated Flight and Propulsion Control Design using $\mathcal{H}^\infty$ Loop-Shaping Techniques," *Proceedings of the IEEE Conference on Decision and Control*, Vol. 2, IEEE Publications, Piscataway, NJ, 1999, pp. 1523–1528.

[7]Bates, D. G., Gatley, S. L., Postlethwaite, I., and Berry, A. J., "Design and Piloted Simulation of a Robust Integrated Flight and Propulsion Controller," *Journal of Guidance, Control, and Dynamics*, Vol. 23, No. 2, 2000, pp. 269–277.

[8]Gatley, S. L., Bates, D. G., and Postlethwaite, I., "A Partitioned Integrated Flight and Propulsion Control System with Engine Safety Limiting," *IFAC Journal of Control Engineering Practice*, Vol. 8, No. 8, 2000, pp. 845–857.

[9]Tischler, M. B. (ed), *Advances in Flight Control*, Taylor and Francis, London, 1996.

[10]Dadd, G. J., Sutton, A. E., and Greig, A. W. M., "Multivariable Control of Military Engines," *Advanced Aero-Engine Concepts and Controls*, CP-572, AGARD, Vol. 28, 1996, pp. 1–12.

[11]Harefors, M., "A Study in Jet Engine Control: Control Structure Selection and Multivariable Design," Ph.D. Dissertation, Dept. of Control Engineering, Chalmers Univ. of Technology, Chalmers, Sweden, 1999.

[12]Samar, R., "Robust Multi-Mode Control of High Performance Aeroengines," Ph.D. Dissertation, Dept. of Engineering, Univ. of Leicester, Leicester, England, U.K., 1995.

[13]Glattfelder, A. H., and Schaufelberger, W., "Stability of Discrete Override and Cascade-Limiter Single-Loop Control Systems," *IEEE Transactions on Automatic Control*, Vol. 33, No. 6, 1998, pp. 532–540.

[14]Postlethwaite, I., Samar, R., Choi, B. W., and Gu, D. W., "A Digital Multi-Mode $\mathcal{H}^\infty$ Controller for the Spey Turbofan Engine," *Proceedings of the European Control Conference*, Vol. 4, European Control Council, Paris, 1995, pp. 3881–3886.

[15]Gilbert, E. G., and Tan, K. T., "Linear Systems with State and Control Constraints: The Theory and Application of Maximal Output Amissible Sets," *IEEE Transactions on Automatic Control*, Vol. 36, No. 8, 1991, pp. 1008–1019.

[16]Rundquist, L., "Anti-Reset Windup for PID Controllers," Ph.D. Dissertation, Dept. of Automatic Control, Lund Inst. of Technology, Lund, Sweden, 1991.

[17]Turner, M. C., and Postlethwaite, I., "The Application of Monotone Stability to Certain Saturated Feedback Interconnections," *Proceedings of the IEEE Conference on Decision and Control*, Vol. 1, IEEE Publications, Piscataway, NJ, 2000, pp. 1081–1086.

[18]Khalil, H., *Nonlinear Systems*, Prentice–Hall, Upper Saddle River, NJ, 1996, pp. 419–423.

[19]Boyd, S., and Yang, Q., "Structured and Simultaneous Lyapunov Functions for System Stability Problems," *International Journal of Control*, Vol. 49, No. 6, 1989, pp. 2215–2240.